iScience, Volume *26*

Supplemental information

A nanobody recognizes a unique conserved epitope and potently neutralizes SARS-CoV-2 omicron variants

Naphak Modhiran, Simon Malte Lauer, Alberto A. Amarilla, Peter Hewins, Sara Irene Lopes van den Broek, Yu Shang Low, Nazia Thakur, Benjamin Liang, Guillermo Valenzuela Nieto, James Jung, Devina Paramitha, Ariel Isaacs, Julian D.J. Sng, David Song, Jesper Tranekjær Jørgensen, Yorka Cheuquemilla, Jörg Bürger, Ida Vang Andersen, Johanna Himelreichs, Ronald Jara, Ronan MacLoughlin, Zaray Miranda-Chacon, Pedro Chana-Cuevas, Vasko Kramer, Christian Spahn, Thorsten Mielke, Alexander A. Khromykh, Trent Munro, Martina L. Jones, Paul R. Young, Keith Chappell, Dalan Bailey, Andreas Kjaer, Matthias Manfred Herth, Kellie Ann Jurado, David Schwefel, Alejandro Rojas-Fernandez, and Daniel Watterson

This file includes
Supplementary information
Supplementary Figures 1 to 15
Supplementary Table 1 to 2

Table S1. Cryo-EM Data collection, processing and refinement statistics (Related to Figure 2)

Wu spike/W25 complex

Magnification	31000
Voltage	300
Total dose per movie stack [e/Å^2]	62
Defocus range [μm]	0.5-2.5
Pixel size [Å]	0.625
Initial particle no.	284399
Final particle no.	76384 (map 1), 56250 (map 2), 132634 (map 3)
Map resolution [Å]	3.80 (map 1), 3.81 (map 2), 5.92 (map 3)
FSC threshold	0.143
Map sharpening B factor [Å^2]	-96.4 (map 1), -94.5 (map 2), -484.1 (map 3)

	Map 3
Starting model	PDB 6dsz
Model fit CCs - mask/box/peaks/volume	0.70/0.82/0.83/0.71
Model resolution - masked/unmasked	6.7/6.6 (5.0/5.1)
FSC threshold	0.5 (0.143)
Model composition	
Protein residues	542
Ligands	BMA:3, NAG:9
Average B factors [Å^2]	
Protein	269.6
Ligand	329.6
R.m.s. deviations	
Bond lengths [Å]	0.003
Bond angles [°]	0.72
Validation	
MolProbity score	2.12
Clashscore	6.27
Poor rotamers [%]	1.5
Ramachandran plot	
Favoured [%]	85.9
Allowed [%]	14.1
Disallowed [%]	0

Omicron spike/W25 complex

Magnification	60000
Voltage	300
Total dose per movie stack [e/Å^2]	40
Defocus range [μm]	0.5-2.5
Pixel size [Å]	0.4
Initial particle no.	222237
Final particle no.	32512 (map 4 and 5)
Map resolution [Å]	4.97 (map 4), 6.04 (map 5)
FSC threshold	0.143
Map sharpening B factor [Å^2]	-189.6 (map 4), -411.8 (map 5)

	Map 5
Starting model	PDB 7wg6
Model fit CCs - mask/box/peaks/volume	0.77/0.91/0.91/0.77
Model resolution - masked/unmasked	6.2/6.2 (4.9/4.9)
FSC threshold	0.5 (0.143)
Model composition	
Protein residues	567
Ligands	BMA:2, NAG:9, MAN:2
Average B factors [Å^2]	
Protein	325.7
Ligand	318.3
R.m.s. deviations	
Bond lengths [Å]	0.003
Bond angles [°]	0.659
Validation	
MolProbity score	2.22
Clashscore	18.16
Poor rotamers [%]	0
Ramachandran plot	
Favoured [%]	92.7
Allowed [%]	7.1
Disallowed [%]	0.2

Table S2. Survey of camelid and synthetic nanobody structures in complex with SARS-CoV2 Spike RBD. (Related to Figure 2E)

NB	Type	Method	PDB ID	Reference PMID
C1	side-1	X-ray	7oap	34552091
C5	top	X-ray	7oao	34552091
H3	top	X-ray	7oap	34552091
F2	side-1	X-ray	7oay	34552091
Nb17	side-2	Cryo-EM	7mej	34344900
Nb21	top	Cryo-EM	7mdw	34344900
Nb36	side-2	Cryo-EM	7mej	34344900
Nb105	side-1	Cryo-EM	7mdw	34344900
VHH E	top	Cryo-EM	7ksg, 7b17	33436526
VHH V	side-1	Cryo-EM	7b11, 7b17	33436526
VHH U	side-1	X-ray	7kn5	33436526
VHH W	side-1	X-ray	7kn7	33436526
Ty-1	top	Cryo-EM	6zxn	32887876
H11-D4	top	X-ray	6yz5	32661423
H11-H4	top	X-ray	6zbp	32661423
NM1226	side-1	X-ray	7nkt	33904225
NM1230	top	X-ray	7b27	33904225
WNb-2	top	X-ray	7ldj	33893175
WNb-10	side-1	Cryo-EM	7lx5	33893175
Re5D06	top	X-ray	7olz	34302370
Re9F06	side-1	X-ray	7olz	34302370
Nb20	top	X-ray	7jvb	33154108
Nanosota-1	top	X-ray	7km5	34338634
MR17 (synthetic)	top	X-ray	7c8w	34330908
SR4 (synthetic)	top	X-ray	7c8v	34330908
SR31 (synthetic)	side-1 (unconventional)	X-ray	7d2z	33657135
Sb16 (synthetic)	top	X-ray	7kgk	34537245
Sb45 (synthetic)	top	X-ray	7kgj	34537245
Sb 68 (synthetic)	side-1	X-ray	7klw	34537245

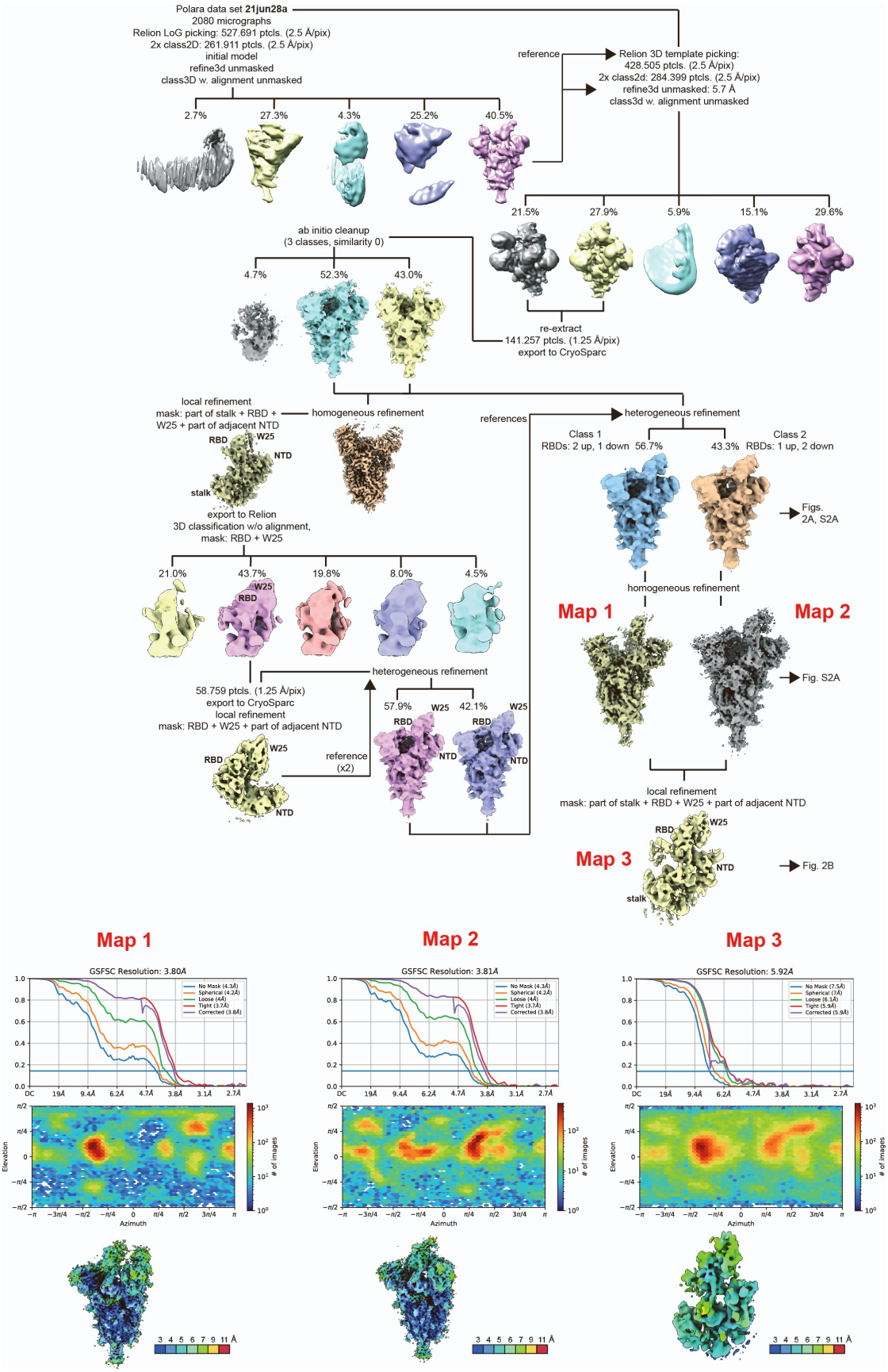

Supplementary Figure 1. Cryo-EM processing scheme for Wu spike/W25. (Related to Figure 2)

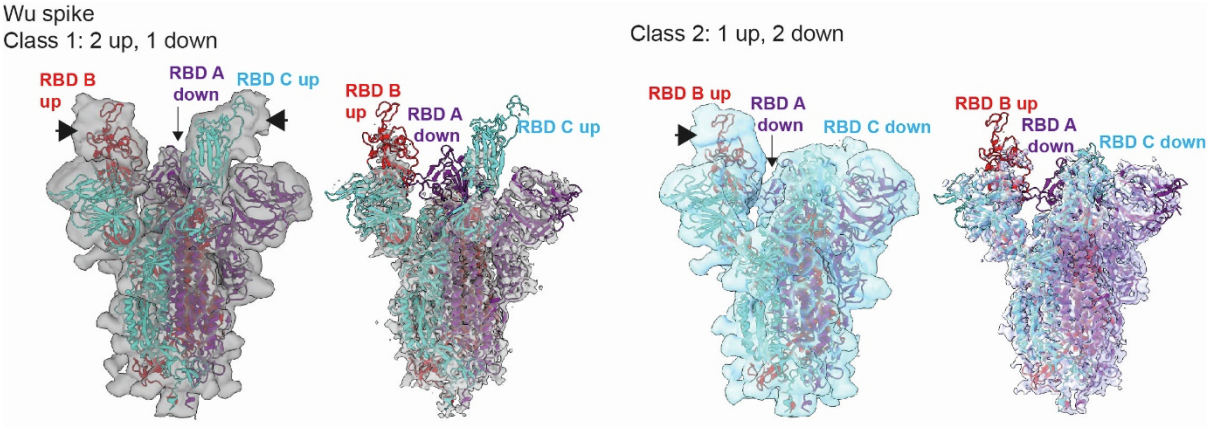

Supplementary Figure 2. Conformational states of the Wu spike/W25 complex. (Related to Figure 2A and B)

Cryo-EM densities representing spike conformational class 1 (grey – map 1 [Fig. S1]) and class 2 (cyan, map 2 [Fig. S1]. The left panel for each class shows a filtered map at higher contour level to better illustrate the extra densities corresponding to W25 (indicated by the black arrows). The spike protein is represented as in Fig. 2A

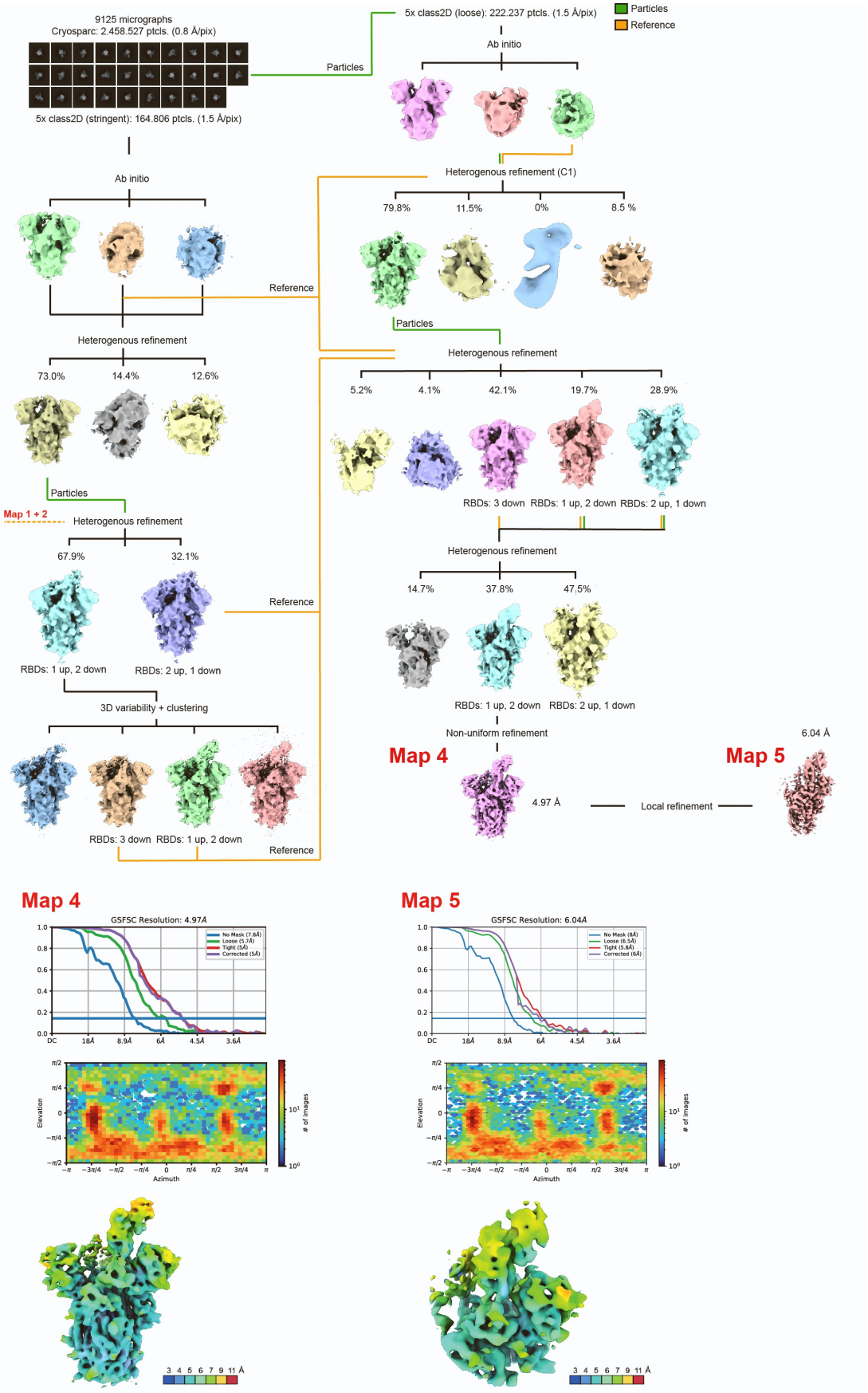

Supplementary Figure 3. Cryo-EM processing scheme for Omicron spike/W25. (Related to Figure 2A and B)

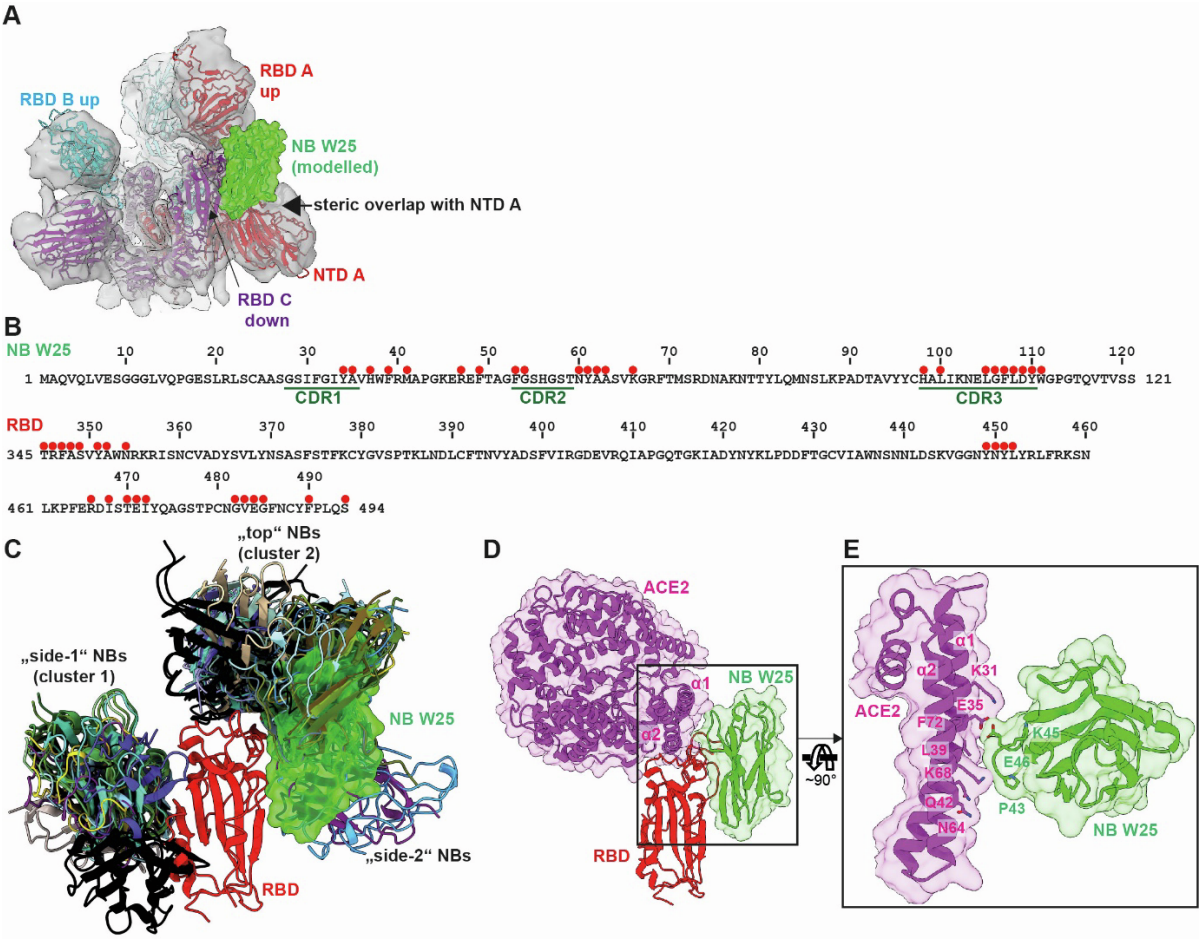

Supplementary Figure 4. Detailed structural analysis of the Wu spike/W25 interaction, comparison to the binding modes of other nanobodies and of the ACE2 receptor. (Related to Figure 2)

(A) Superposition of a W25-bound RBD with the "down"-RBD of the spike trimer. A steric clash between the modelled W25 position and the adjacent NTD is indicated by the arrow. **(B)** Upper panel: amino acid sequence of W25. All amino acid residues involved in molecular contacts with the spike RBD, including main chain interactions, are indicated as red dots above the sequence. CDRs are underlined. Lower panel: Amino acid sequence of spike RBD (original Wuhan isolate). All amino acid residues involved in molecular contacts with the spike RBD are indicated as red dots above the sequence. **(C)** Superposition of all camelid and synthetic nanobody/SARS-CoV2 RBD structures available in the PDB (Table S1). Only the RBD of PDB entry 7oap (red cartoon) is shown for clarity. Nanobodies are shown in cartoon representation, and nanobody W25 additionally as semi-transparent surface.**(D)** Superposition of the spike RBD/ACE2 receptor complex (PDB 7a94, (Benton et al., 2020) with the RBD/nanobody W25 structure. For clarity, only the RBD of the W25 complex is shown as red cartoon. ACE2 (magenta) and W25 (green) are depicted as cartoons together with a semi-transparent representation of their solvent-accessible surfaces. **(E)** Detailed view of the structural superposition from H. Selected ACE2 (magenta) and W25 (green) amino acid side chains are shown in stick representation.

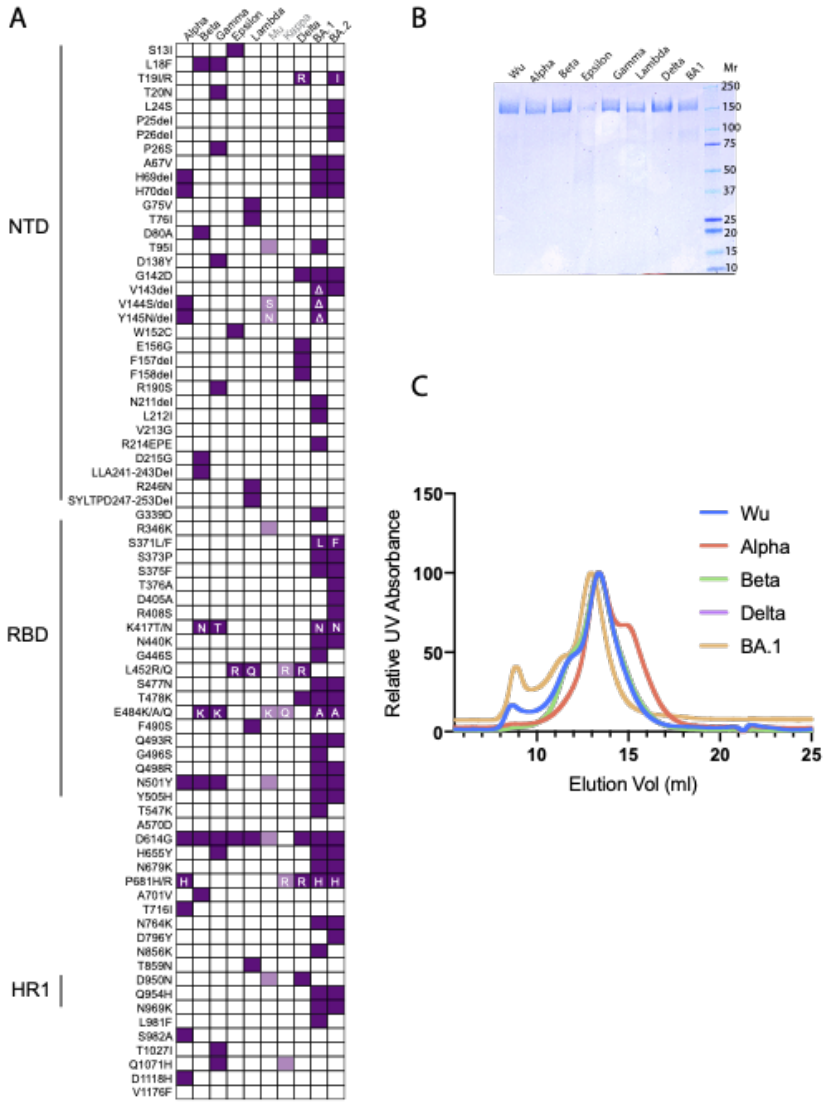

Supplementary Figure 5. Mutations in VOC spike proteins and characterisation of the spike preparations. (Related to Figure 3)

(A) Mutations as labelled in purple were introduced in spike proteins. The black-colored spike variants are included in this study, the grey-colored ones not. **(B)** The proteins were affinity purified, concentrated and buffer exchanged into PBS pH 7.4. Two micrograms of each protein were prepared in 4X lysis buffer, boiled and reduced. Proteins were loaded on SDS-PAGE and visualised using Coomassie Blue staining indicating pure purified spike protein. **(C)** Size exclusion chromatography profiles of purified spike proteins (Superose 6 Increase 10/300 column).

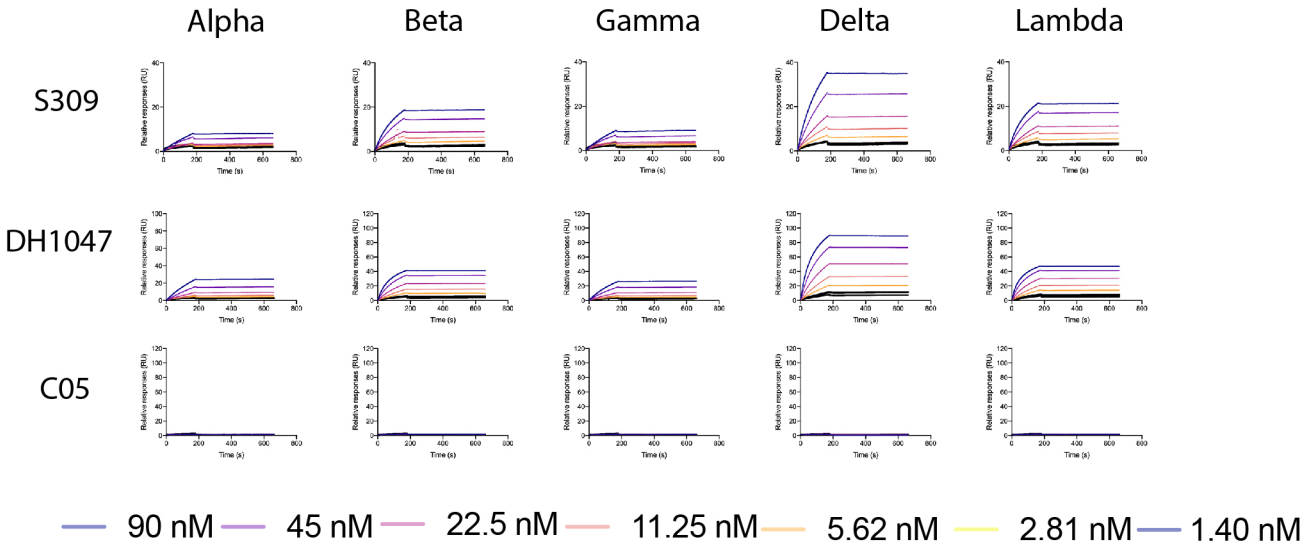

Supplementary Figure 6. SPR sensorgrams of S309, DH1047 and C05. (Related to Figure 3A and B)

mAbs were immobilized on SPR protein A chips. Various concentrations of SARS-CoV-2 spike variant proteins as indicated were injected for 180 s, followed by dissociation for 600 s. Dissociation constants (K_D) were determined on the basis of fits, applying a 1:1 interaction model. Dissociation constants (K_D) were determined based on fits, applying a 1:1 interaction model.

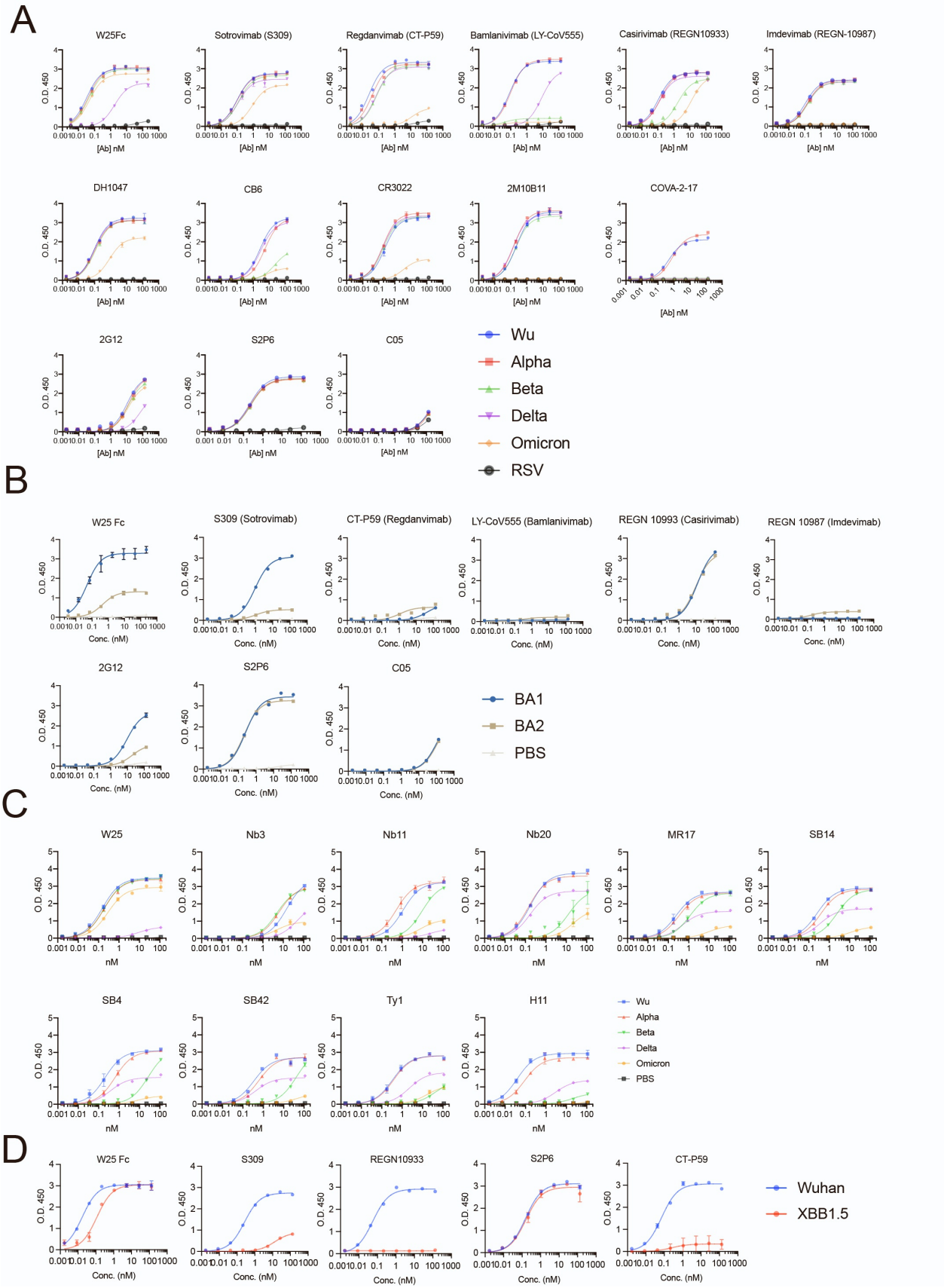

Supplementary Figure S7. ELISA binding curves of W25Fc, EUA mAbs other epitope specific mAbs to SARS-CoV-2 Spikes variants. (Related to Figure 3)

(A) Binding curves of W25Fc, S309, CT-P59, REGN-10933, REGN-10987, DH1047, CB6, CR3022, 2M10B11, COVA2-17, 2G12, S2P6 and C05 (control mAbs) to Wu, Alpha, Beta, Delta and Omicron (BA.1). **(B)** Binding curves of W25Fc, S309, CT-P59, REGN-10933, REGN-10987, 2G12, S2P6 and C05 (control mAbs) to BA.1 and BA.2. **(C) B**inding curves of W25Fc, Nb3, Nb11, Nb20, MR17, SB14, SB4, SB42, Ty1, H11 to Wu-1, Alpha, Beta, Delta and Omicron (BA.1) demonstrating that W25 Fc binds Omicron spike whereas other Nbs lost their affinities to Omicron spike. (D) Binding curves of W25Fc, S309, CT-P59, REGN-10933 and S2P6 against Wuhan and XBB.1.5 spike proteins.

Data are generated from two- three independent experiments, each performed in technical duplicate. Error bar indicates SEM.

A

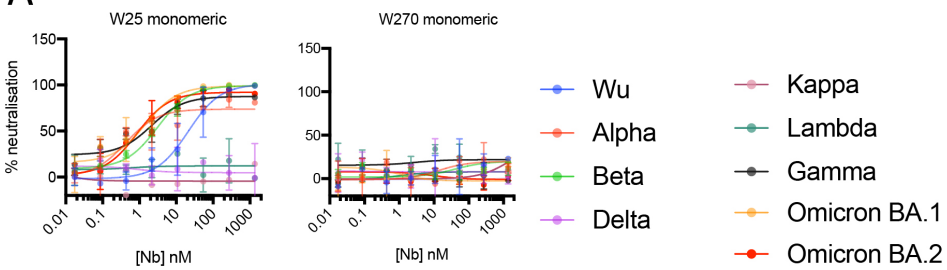

B

Domain	IC_{50} (nM±SEM)								
	Wu	Alpha	Beta	Gamma	Kappa	Delta	Lambda	BA.1	BA.2
W25	22.63±7.97	0.42±0.22	2.10±0.35	2.12±0.98	-	-	-	0.62±0.22	0.85±0.26
W270	N/A	N/A	N/A	N/A	N/A	N/A	N/A	N/A	N/A

Supplementary Figure 8. Live virus neutralisation assay of W25 Nb against SARS-CoV-2 Wu and VOCs. (Related to Figure 3D and E) **(A)** Neutralisation curves comparing the sensitivity of SARS-CoV-2 strains (Alpha, Beta, Delta, Kappa, Lambda, Gamma) to W25 Nb, control Nb (W270) as indicated. Live SARS-CoV-2 virus different variants were incubated with serially diluted mAbs, in duplicate, for 1 hour at 37C, and then used to infect Vero E6 cells. After 30 mins, overlay media were added. Twenty hours post-infection, overlays were removed, cells were fixed with cold 80% acetone and dry prior staining for foci. The data were analysed and plotted using nonlinear regression (curve fit, three parameter) and IC_{50} value was calculated from neutralisation curve by Graphpad Prism 8 software. Color represents SARS-CoV-2 variants.

(B) Summary of IC_{50} values (nM) of neutralisation of SARS-CoV-2 variants performed in VeroE6 cells. Values that approached 50% neutralization were estimated from (A).

Data are generated from two independent experiments, each performed in technical duplicate. Error bar indicates SEM.

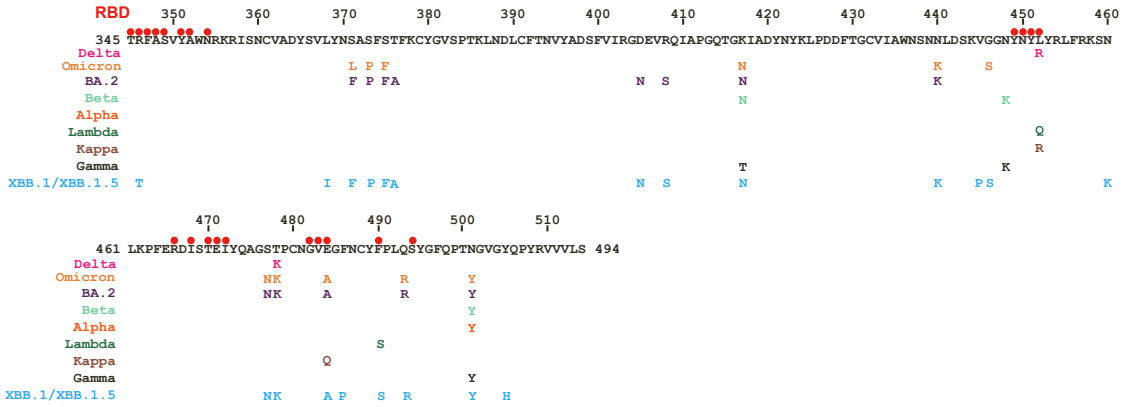

Supplementary Figure 9. Amino acid residues on spike RBD involved in molecular contacts with W25. (Related to Figure 3F)

Interacting residues are indicated as red dots above the sequence. Positions mutated in the SARS-CoV2 variants are shown in the sequence.

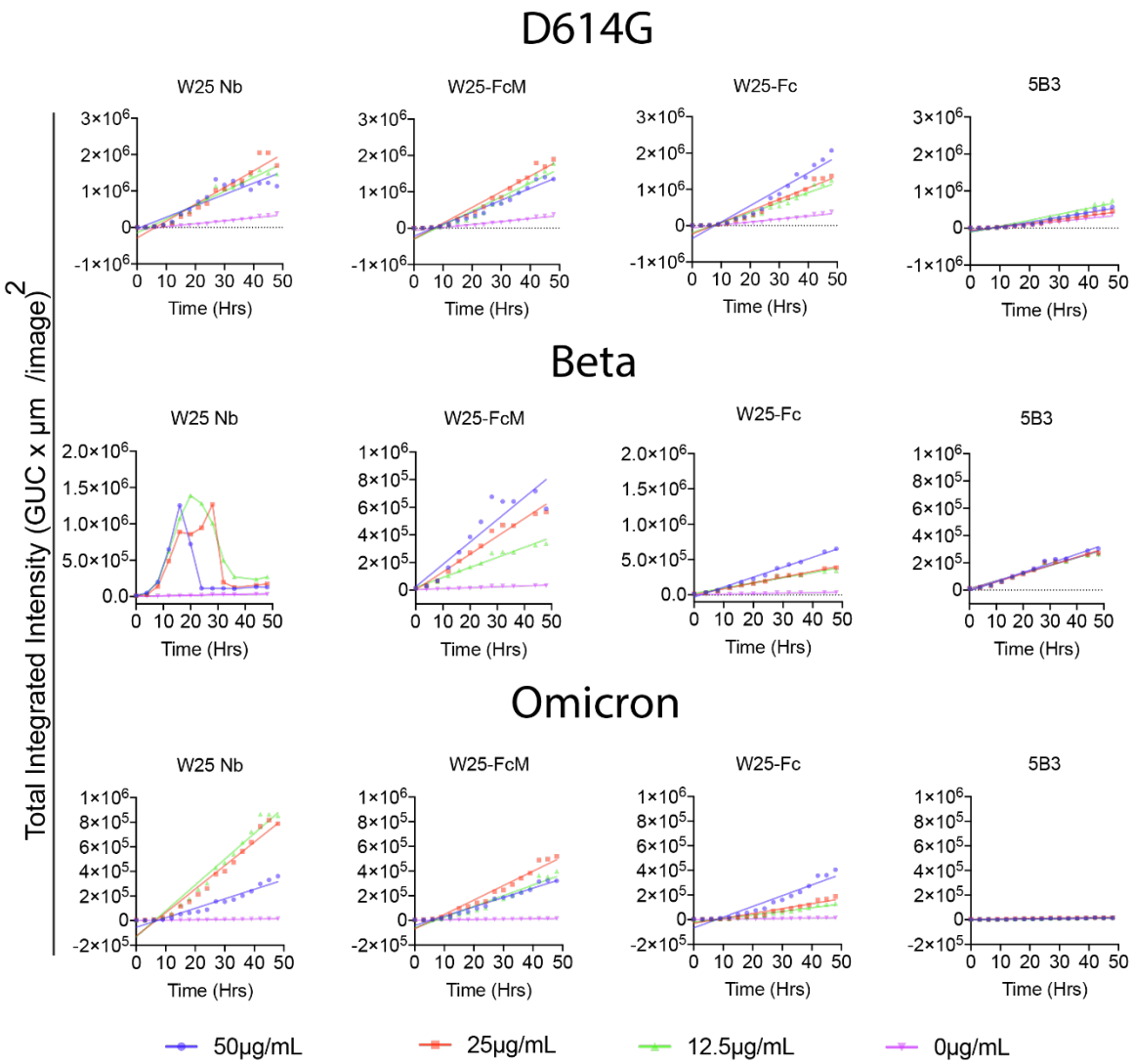

Supplementary Figure 10. Cell-cell fusion assay of SARS-CoV-2 spike. (Related to Figure 3G)

W25 enhances spike-mediated cell fusion monitored by GFP-positive syncytia cells. The data plotted shows the total sum of syncytia fluorescent intensity in the image, calculated used the total integrated intensity metric and expressed as green count units (GCU) per μm^2. W25, its derivatives and control antibody were diluted to the indicated concentrations and subsequently incubated with 2×10^4 effector cells in 50 µl at 37 °C, 5% CO_2 for 1 h. The W25 Nb, W25-FcM, W25-Fc, 5B3 (as control) and effector cell mixture were then subjected to incubation with target cells in corresponding wells and incubated for 18–24 h. GFP-positive syncytia were imaged every hour using the IncuCyte S3 live cell imaging system (Essen BioScience). Five fields of view were taken per well at 10× magnification, and GFP expression was determined using the total integrated intensity metric included in the IncuCyte S3 software (Essen BioScience). Representative images are illustrated in fig.S11.

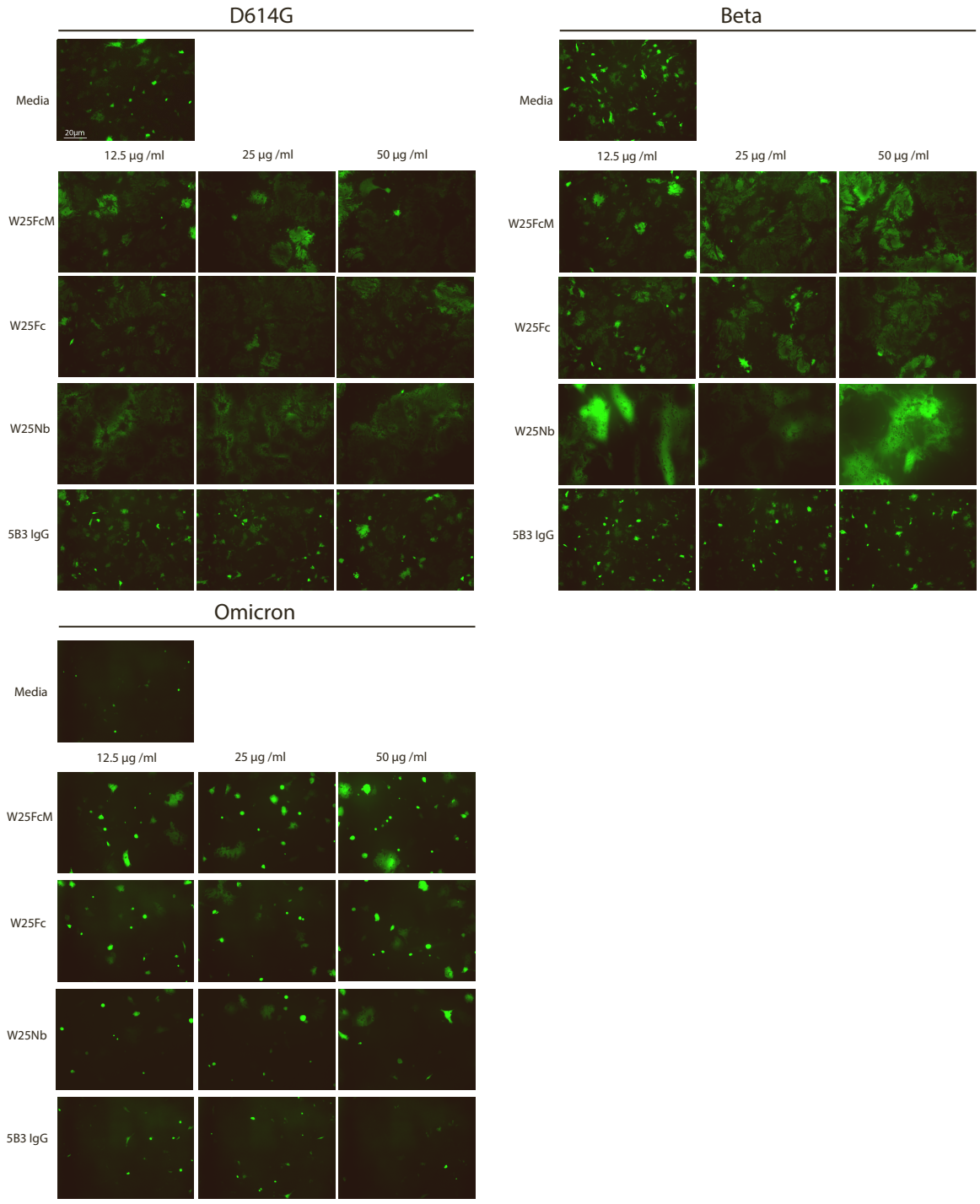

Supplementary Figure 11. Representative images illustrating GFP-positive syncytia from cell-cell fusion corresponding to Fig. S10. (Related to Figure 3G)

Cells were transfected with **(A)** SARS-CoV-2 D614G, **(B)** Beta and **(C)** Omicron variant spikes .

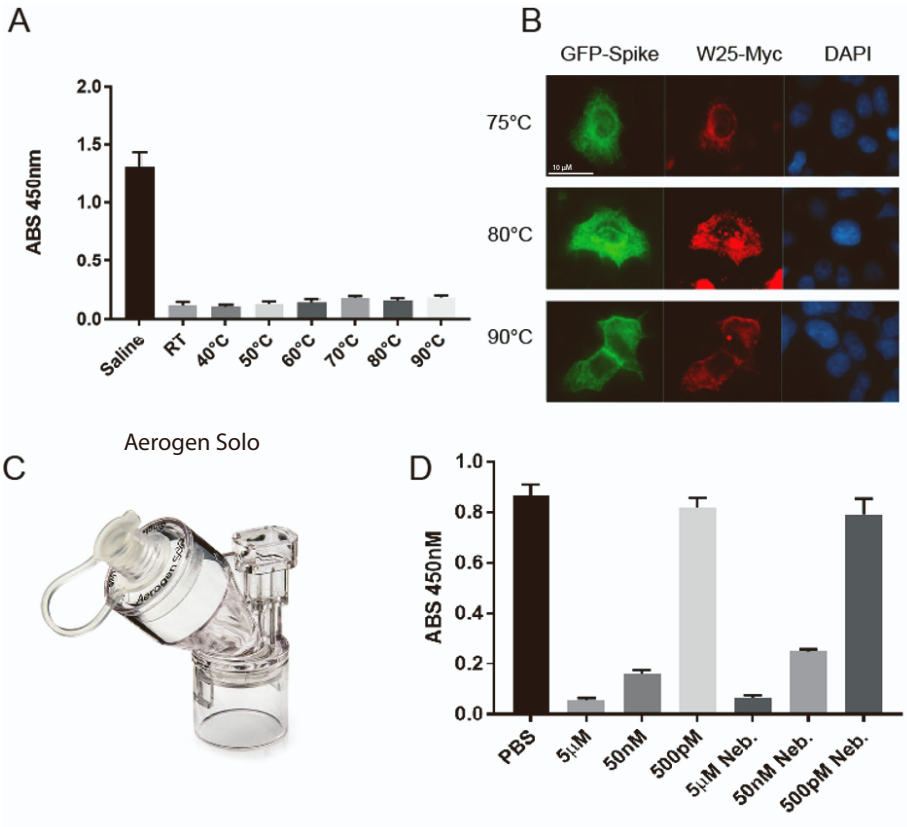

Supplementary Figure 12. Thermostability and nebulisation stability of W25. (Related to Figure 4)

(A) Competition ELISA assay. RBD was immobilised on ELISA plates and W25, covalently modified with HRP, was added in the presence or absence of untagged W25, which was heat-treated for 20 min at the indicated temperatures. **(B)** Immunofluorescence of Hela cells transient transfected with GFP-Spike using heat-treated myc tagged W25 (red). **(C)** Aerogen Solo nebulizer used for W25 Nebulisation in PBS. **(D)** Competition ELISA as in A, using decreasing amounts of W25 or W25 post-nebulisation.

Data are generated from two independent experiments, each performed in technical duplicate.

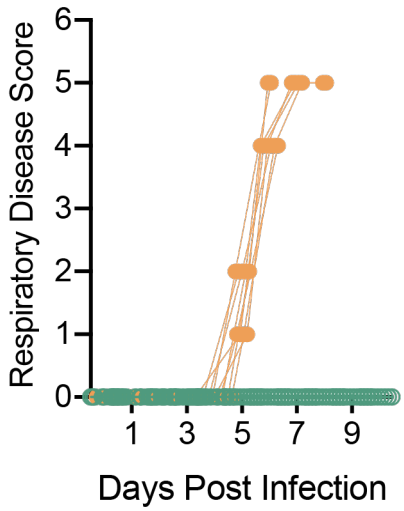

Supplementary Figure 13. Respiratory disease scores of K18-hACE2 mice infected with SARS-CoV-2 Beta variant and received W25-Fc 4 h prior to infection. (Related to Figure 4A-E)

Respiratory disease scores of SARS-CoV-2 Beta infected mice (Fig. 4A-E).

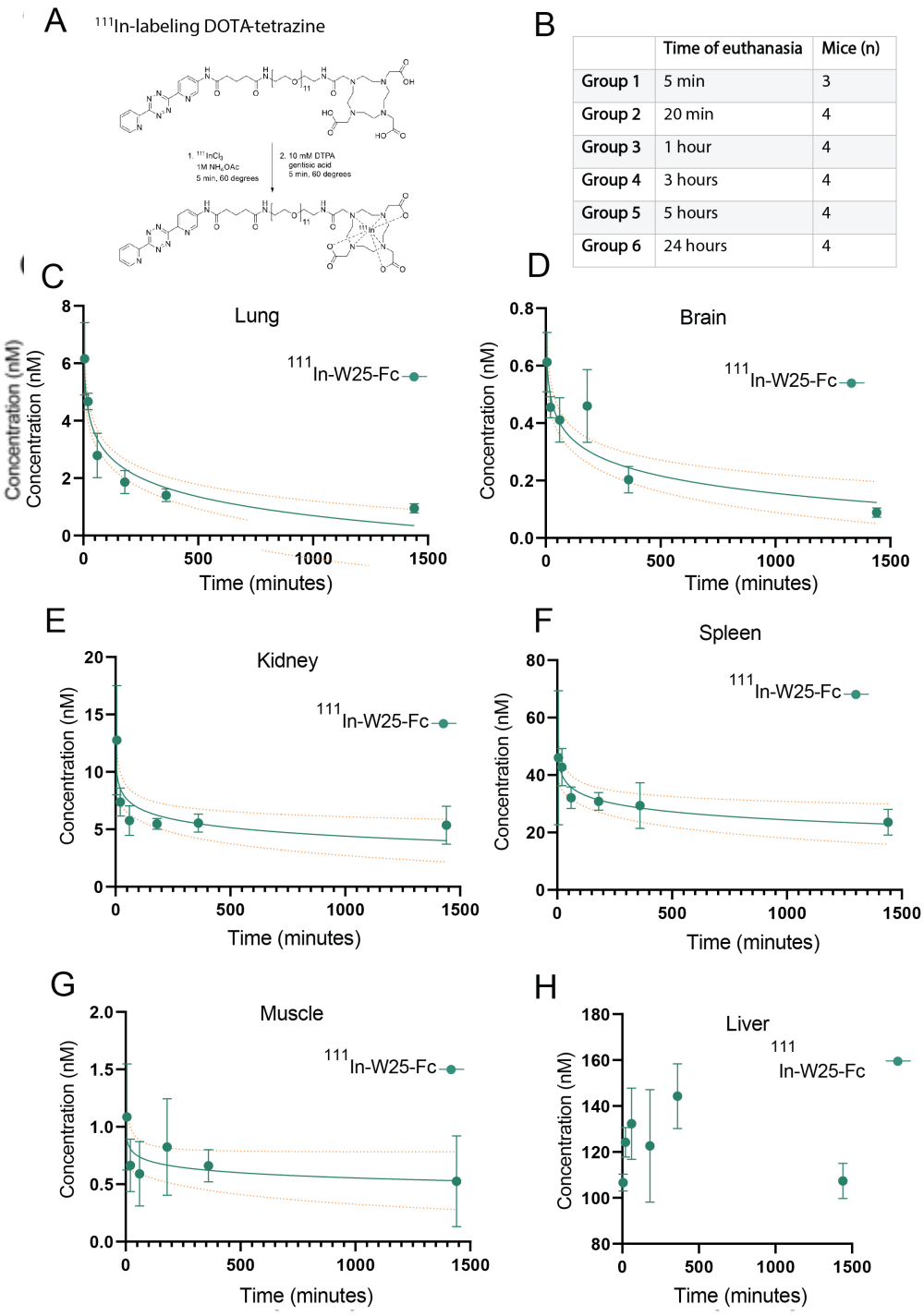

	Time of euthanasia	Mice (n)
Group 1	5 min	3
Group 2	20 min	4
Group 3	1 hour	4
Group 4	3 hours	4
Group 5	5 hours	4
Group 6	24 hours	4

Supplementary Figure 14. Pharmacokinetic of ^{111}Indium radiolabelled W25-Fc. (Related to Figure 4T)
(A) Conjugation of W25-Fc was conjugated to radioactive ^{111}Indium.
(B) ^{111}Indium W25-Fc (1 mg/kg) was injected intravenously via the tail to 6 groups of mice (group 1: 5 min, group 2: 20 min, group 3: 60 min, group 4: 3 hr, group 5: 5 hr and group 6: 24 hr). The mice were dissected and concentration of ^{111}In W25 was measured the following tissues using an Auto-Gamma Counter: **(C)** Lung, **(D)** Brain, **(E)** Kidney, **(F)** Spleen, **(G)** Muscle and **(H)** Liver. Error bar indicates SEM from different mice.

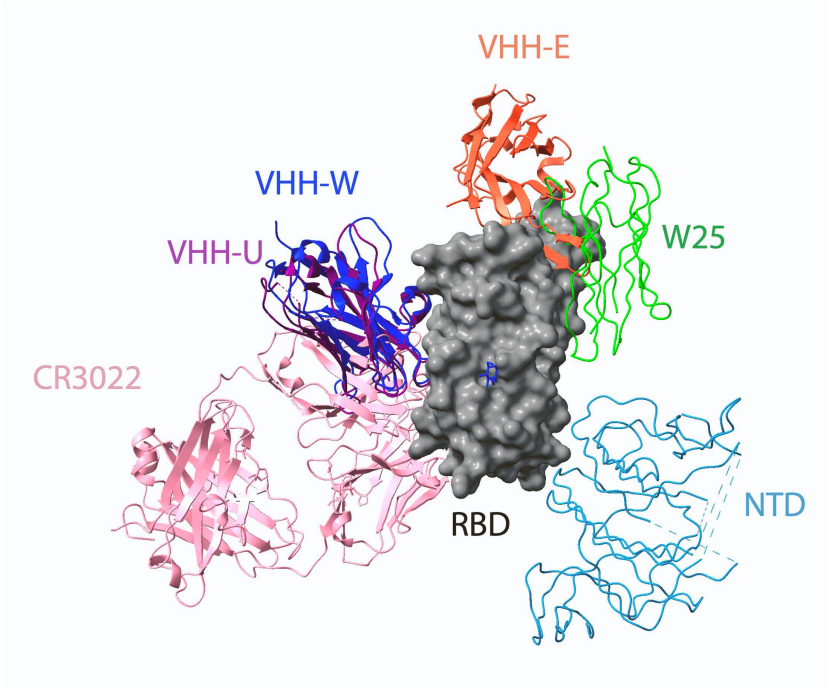

Supplementary Figure 15. Structural comparison of antibodies and nanobodies that induce unconventional neutralisation mechanism (Related to Discussion in main text)
W25, VHH W (PDB 7KN7), U (7KN5), and E (7KN5), and mediating spike disruption: CR3022 (6W41).